INSTITUTE OF PHYSICS PUBLISHING JOURNAL OF PHYSICS D: APPLIED PHYSICS

J. Phys. D: Appl. Phys. **34** (2001) 2825–2829 PII: S0022-3727(01)24468-4

Evaluation of the relaxation parameters of interfacial polarization processes in calcite containing dolomite and quartz inclusions by TSDC spectroscopy

A N Papathanassiou

Solid State Physics Section, Department of Physics, University of Athens, Panepistimiopolis, GR 157 84 Zografos, Athens, Greece

Received 2 May 2001, in final form 3 July 2001
Published 5 September 2001
Online at stacks.iop.org/JPhysD/34/2825

Abstract

The pre-exponential factor of an Arrhenius-type temperature dependence of the relaxation time of the interfacial polarization processes is sensitive to the size distribution and the orientation of (conductive) inclusions. An alternative narrow-window thermal sampling thermally stimulated depolarization currents (TSDC) procedure was applied in order to decompose two different overlapping mechanisms of interfacial polarization in a calcite matrix accommodating a random distribution of quartz and dolomite inclusions, which are more conductive than the host. The distribution of the activation energy and the pre-exponential factors were obtained from the analyses of the TSDC constituents. The orders of magnitude of the relaxation times agree with those predicted theoretically. The distributions in the values of the activation energy and the pre-exponential factor are discussed with respect to predictions of the theory for conductive ellipsoids dispersed in an insulating matrix.

1. Introduction

The calcite family consists of magnesite ($MgCO_3$), calcite ($CaCO_3$) and the mixed crystal dolomite ($CaMg(CO_3)_2$) [1]. These compounds all crystallize in the rhombohedral system and may be described approximately by the sodium chloride structure, regarding the cubic unit cell suppressed along its diagonal axis. A potential departure from the sodium chloride structure approximation is that the carbonate group is not a centre of symmetry, since the three oxygens in magnesite and calcite settle at the corners of an equilateral triangle, and the carbon settles at its centre [2]. Slight distortions and deviations from the aforementioned picture preserve the structural stability of the mixed crystal dolomite [2].

Thermally stimulated depolarization currents (TSDC) studies [3] in the calcite group members were recently carried out, aimed at the understanding of the preferential formation of certain polarizable defect centres upon the specific lattice type [4–8]. Two TSDC peaks have been detected in single crystal calcite: one is located at 188 K and is attributed to the rotation of defect dipoles; the other is at about 230 K, which might be attributed to the localized hopping within the quartz inclusions [7]. The transport properties were also studied by means of TSDC experiments [9, 10]. The long-distance charge transport yields space charge polarization in dolomite [9], while trapping occurs in homogeneously spatially distributed traps in magnesite [10].

The presence of different conductive inclusions in calcite, with adjacent electrical and dielectric features yield interfacial polarization processes with like relaxation parameters. The problem of thermally stimulated depolarization stemming from ellipsoidal particles in an insulating medium was treated through computer simulation [11]. Such peaks are characterized by a distribution in the pre-exponential factor τ_0. In the present work, we intend to use the thermal sampling TSDC scheme so as to resolve double interfacial polarization processes and obtain the distribution of the activation energy and the pre-exponential factor values by analysing the particular sampling components.

2. Theory

The polarization processes related to interfacial phenomena (known as Maxwell–Wagner–Sillars polarization) occurring in insulators containing conductive inclusions are governed by a relaxation time, which was proposed by Sillars, see [11–13]:

$$\tau = \varepsilon_0 \frac{(n_i - 1)\varepsilon_1 + \varepsilon_2}{\sigma_2} \tag{1}$$

where ε_0 is the permittivity of free space, n_i is a geometrical factor depending on the shape of the inclusions and their orientation with respect to the polarizing field, ε_1 and ε_2 denote the (static) dielectric constants of the matrix and the inclusions, respectively, and σ_2 is the conductivity of the (semiconductive) inclusions. The latter equation is valid under the restriction that the conductivity of the matrix σ_1 is considerably smaller than σ_2. n_i holds a unique value (labelled n) provided that the inclusions are identical and have the same axes oriented along the direction of the polarizing electric field. Note that $n = 3$ for spherical inclusions.

Assuming that a thermally activated conductivity mechanism operates within the inclusions, we may assert that

$$\sigma_2(T) = \sigma_0 \exp(-E/kT) \tag{2}$$

where k is the Boltzmann constant, σ_0 is a pre-exponential factor and E denotes the activation energy. From (1) and (2), the relaxation time takes the form of an Arrhenius equation:

$$\tau(T) = \tau_0 \exp(E/kT) \tag{3}$$

where the pre-exponential factor τ_0 is

$$\tau_0 = \varepsilon_0 \frac{(n - 1)\varepsilon_1 + \varepsilon_2}{\sigma_0}. \tag{4}$$

The TSDC signal that corresponds to the interfacial phenomena resembles that obtained for rotating dipoles [3]:

$$I(T, E) = \frac{S\Pi_0}{\tau_0} \exp\left[-\frac{E}{kT} - \frac{1}{b\tau_0} \int_{T_0}^{T} \exp\left(-\frac{E}{kT'} \right) \mathrm{d}T' \right] \tag{5}$$

where Π_0 is the initial polarization of the dielectric, S is the sample's surface area which is in contact with each one of the electrodes, b is a constant of the heating rate and T_0 is identical to the liquid nitrogen temperature (*LNT*).

The direct applicability of equation (5) for the analysis of the TSDC signals produced by interfacial polarization mechanisms is constrained by (4); τ_0 is not single valued but is sensitive to the size distribution and the orientation (with respect to the direction of the polarizing field) of the conducting inclusions [11]. Since the distribution in τ_0 may not be prescribed, it is necessary to resolve experimentally the TSDC peak into a finite set of elementary components. To a first approximation, a particular component may be described by a single τ_0 value, while E may be assumed to obey a normal distribution around E_0 with broadening parameter σ:

$$f(E) = \frac{1}{\sqrt{2\pi}\sigma} \exp\left[-\frac{(E - E_0)^2}{2\sigma^2} \right]. \tag{6}$$

The TSDC current is [14]

$$I(T) = \int_{-\infty}^{+\infty} f(E) I(T, E)\, \mathrm{d}E \tag{7}$$

where $I(T, E)$ denotes the single relaxation time function of equation (5).

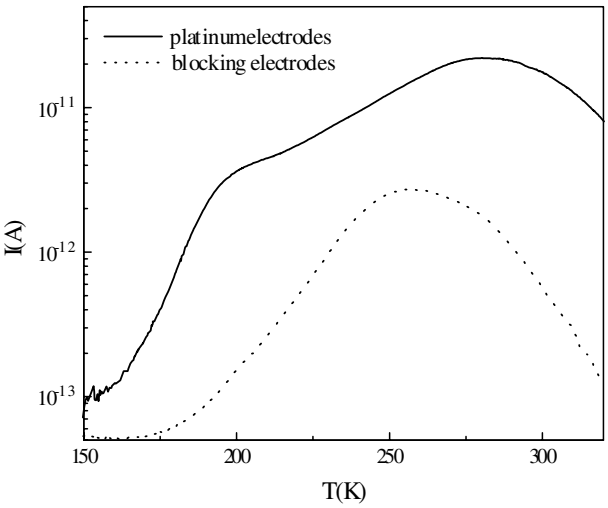

Figure 1. The thermogram of calcite containing quartz and dolomite inclusions obtained by polarizing at $T_p = 298$ K using platinum electrodes (full curve) and insulating spacers (broken curve).

3. Experiment

The TSDC apparatus was described in [15]. The heating rate was $b = 0.045$ K s^{-1}. The composition of the natural polycrystalline samples was: 97 wt% calcite ($CaCO_3$), 3 wt% dolomite ($CaMg(CO_3)_2$) and 1 wt% quartz (SiO_2).

4. Results and discussion

4.1. Decomposition of the TSDC spectrum

A thermogram obtained by employing platinum electrodes together with another one recorded with blocking (Teflon) electrodes is depicted in figure 1. In both cases the sample was polarized at $T_p = 290$ K. The intense band exhibiting its maximum at $T_m = 272$ K is compressed by the use of the blocking electrodes and a peak, which was initially masked by its high-temperature neighbouring relaxation, with its maximum at 256 K is revealed at the expense of the 272 K peak, which is suppressed by the use of insulating spacers. A 'shoulder' observed in the thermogram recorded using platinum electrodes gives evidence for another relaxation mechanism. It is evident that undesirable space charge relaxation occurs close to room temperature. However, the strong overlap among the relaxation mechanisms prohibits the detection of the separate polarization components.

The dielectric relaxation spectrum was decomposed to its constituents by an alternative of the well known thermal sampling scheme [16–18], which consists of polarizing a sample for a short time interval $t_p = 15$ s at constant temperature T_p, which is located within the temperature range where a broad TSDC peak appears, and subsequent abrupt cooling to the *LNT* in the absence of the external polarizing field [19, 20]. By polarizing at T_p for a short time, the slow relaxation mechanisms, which activate at much higher temperatures than T_p, remain practically unpolarized, while the subsequent cooling in the absence of an external polarizing field results in the depolarization of the fast relaxation mechanisms, which activate at temperatures much

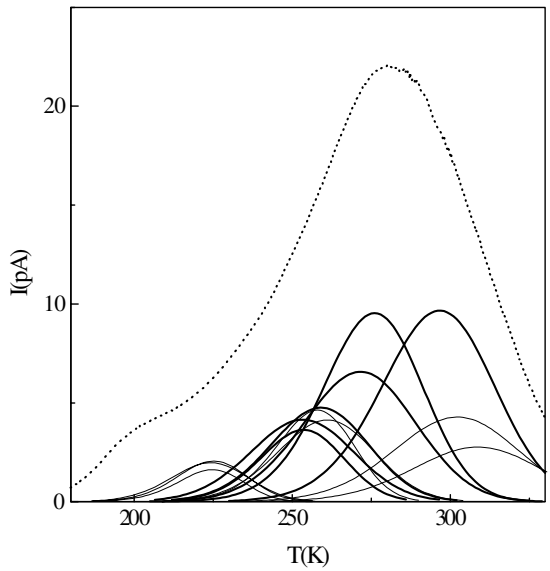

Figure 2. The thermal sampling signals (full curves) together with the thermogram obtained by the conventional TSDC scheme (broken curve).

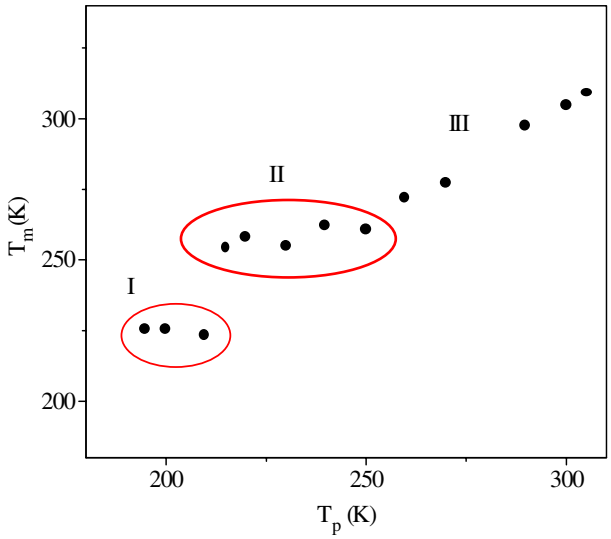

Figure 3. The temperature T_{max} where the thermal sampling peaks reach their maxima against the polarization (sampling) temperature T_p.

Table 1. The temperature T_m where a thermal sampling peak reaches its maximum, together with the relaxation parameters (E_0, σ and τ_0) obtained from the fitting of a theoretical curve with a Gaussian distribution in the activation energy to the experimental data.

Thermal sampling peak	T_m (K)	E_0 (eV)	σ (eV)	τ_0 (s)
I1	225.0	0.576	0.018	2.39×10^{-11}
I2	225.1	0.591	0.022	8.26×10^{-12}
I3	223.2	0.592	0.026	6.19×10^{-12}
II1	254.0	0.650	0.025	1.34×10^{-11}
II2	258.2	0.650	0.021	3.18×10^{-11}
II3	255.1	0.650	0.035	2.82×10^{-11}
II4	262.1	0.660	0.031	2.05×10^{-11}
II5	260.5	0.650	0.031	4.54×10^{-11}
III1	272.3	0.680	0.037	5.35×10^{-11}
III2	277.4	0.680	0.030	2.09×10^{-11}
III3	297.7	0.690	0.032	6.54×10^{-10}
III4	304.5	0.700	0.037	9.32×10^{-10}
III5	309.0	0.710	0.038	6.92×10^{-10}

lower than T_p. Hence, the mechanisms proceeding in the immediate neighbourhood of T_p reach a detectable polarization state, which is detected as a peak in the TSDC spectrum. This alternative selective polarization mode is equivalent to a very narrow windowing sampling and has been applied successfully in many cases where the dielectric spectrum was too complicated [9, 10, 15, 21]. Platinum electrodes were employed in the thermal sampling experiments. The thermal sampling signals are presented in figure 2.

The temperature T_m where a thermal sampling peak reaches a maximum as a function of the (thermal sampling) polarization temperature T_p is depicted in figure 3. It seems that the maxima are likely to distribute over three distinct relaxation mechanisms. The position of the peaks belonging to relaxation I is practically independent of T_p. The dispersion is broader for relaxation II, ranging from 254 to 262 K (table 1). The signals were analysed in terms of the model of the normal distribution in the activation energy around a central value E_0 (equation (7)). The results are presented in table 1. In figure 4, E_0 is plotted as a function of the temperature T_m. The broadening parameter σ is represented by vertical bars. In this diagram it is clear that three different responses constitute the dielectric spectrum. The latter verifies the picture of three relaxations resulting from the $T_m(T_p)$ diagram (figure 3). The corresponding values of the pre-exponential factors τ_0 are presented against T_m in figure 5. Relaxation I is likely to correspond to the 'shoulder' appearing in the thermogram of figure 1. The thermal sampling responses of dispersion II (figure 4) maximize around 259 K and may well be attributed to the band observed at 256 K when blocking electrodes are used (see figure 1).

4.2. Attribution of the relaxation mechanisms

The dramatic reduction of the high-temperature TSDC signal (see figure 1) when blocking electrodes (metal insulator sample insulator metal (MISIM) structure [22]) are employed indicates that the relaxation occurring close to room temperature stems from the annihilation of the (undesirable) space charge. The set of the thermal sampling responses grouped under III, originate from the time reduction of a space charge polarization attained through the migration of free charge carriers along the volume of the specimen and their subsequent trapping close to the sample–electrode interface. The use of insulating electrodes prohibits any discharge on the standard metal electrodes. Hence, the rapid accumulation of the charges close to the electrodes induces an internal electric field that competes with the externally applied field. As a result, the TSDC signal is drastically depressed.

Concerning relaxations I and II, the maxima of the thermal sampling signals depend slightly (negligibly) upon the polarization temperature, as can be seen in figure 3. Both relaxations are of dipolar nature and correspond to the short-range localized hopping of charge carriers. In order to ascertain that they are related to the polarization of the conductive

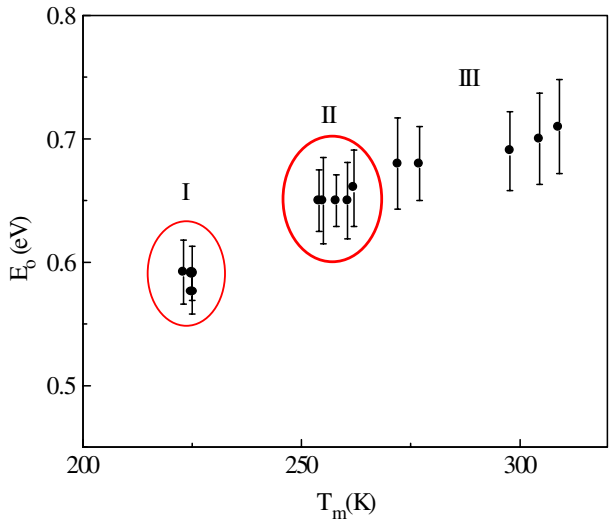

Figure 4. The central values of the activation energy values E_0 against the maxima T_m of the thermal sampling responses. The length of the vertical bars equals 2σ, where σ is the broadening parameter of the Gaussian distribution of the activation energy values around E_0.

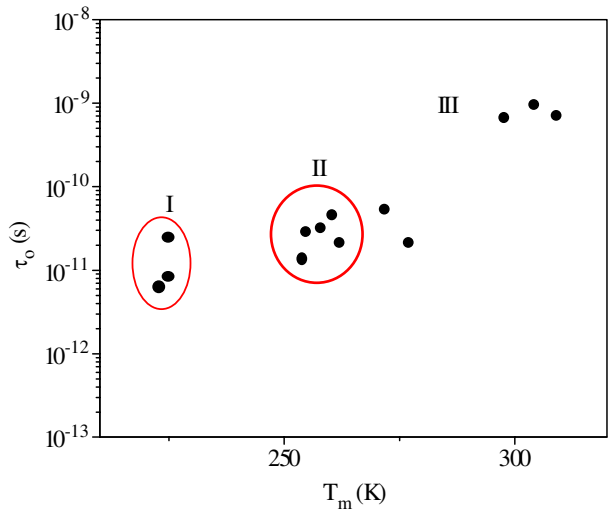

Figure 5. The pre-exponential factor τ_0 against the maxima T_m of the thermal sampling responses.

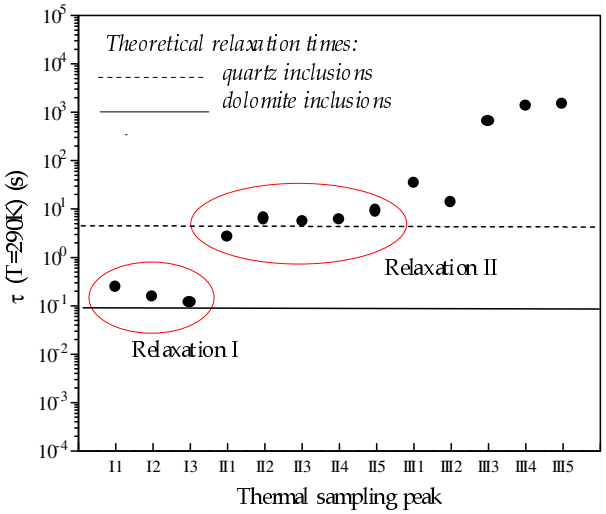

Figure 6. The relaxation time at room temperature obtained using the parameters E_0 and τ_0 which were evaluated from the analyses of the thermal sampling responses. The horizontal lines indicate the relaxation times predicted from the Sillars model.

phases, which are embedded in the calcite matrix, we estimated the relaxation times at room temperature according to equation (1). Their coincidence with the relaxation times (reduced to the room temperature) calculated from the TSDC results, would identify each relaxation mechanism with a specific type of interfacial polarization. The resistivity of the host calcite at room temperature, 5.0×10^{12} Ω m [23], is significantly larger that that of quartz (3.8×10^{10} Ω m [23]) and dolomite ($\approx 10^9$ Ω m [24]). It is expected that interfacial polarization might well occur within such conductive inclusions. Typical values of the static dielectric constants of calcite, quartz and dolomite are 8, 5 and 7, respectively [23]. Recalling that the conductivity is defined as the inverse of the resistivity, by replacing the above mentioned values in (1) and regarding the shape factor $(n-1)$ to be of the order of unity, we get the relaxation time at room temperature: 4×10^0 s for the quartz inclusions and 1×10^{-1} s for the dolomite inclusions. By using the values of E_0 and τ_0, which were obtained from the analyses of the thermal sampling peaks, we calculated the relaxation time τ at room temperature ($T = 290$ K) through the Arrhenius equation (equation (3)). The room-temperature relaxation times corresponding to each relaxation component are depicted in figure 6. In this diagram the two horizontal lines correspond to the relaxation times predicted through the Sillars model (equation (1)). This picture directs one to the interconnection of relaxation mechanisms I and II with the presence of dolomite and quartz inclusions, respectively.

The analyses of the thermal sampling signals showed that both E and τ_0 are distributed. The distribution in τ_0 reflects the distribution in size and orientation of the dispersed inclusions, as mentioned in section 2. The distribution in E could not be prescribed and reflects the operation of multiple conduction mechanisms in the conductive phase. This result could only be obtained by a narrow-window thermal sampling decomposition, since a relaxation mechanism with distribution in both E and τ_0 requires an over-parameterized fitting procedure.

5. Conclusions

Closely separated relaxation mechanisms in calcite containing two dispersed phases of quartz and dolomite, which are more conductive than the host matrix, were decomposed by the thermal sampling TSDC spectroscopy. The relaxation times predicted from the theory of Sillars are compatible with those obtained experimentally, identifying two relaxation mechanisms with the interfacial polarization of the quartz and dolomite inclusions, respectively. The necessity for dielectric relaxation mapping stems from the strong overlap of the interfacial polarization mechanisms (due to their neighbouring relaxation time values) and from the inadequacy of the theory to propose a generalized TSDC equation originating from the polarization of dispersed conductive phases. The values

of the pre-exponential factor are distributed, reflecting the distribution in size and orientation of the inclusions. The activation energy values obey a normal distribution around a mean value, indicating the coexistence of multiple conduction mechanisms within the conductive phases.

References

[1] Deer W A, Howie R A and Zussman J 1996 *An Introduction to the Rock Forming Minerals* (Essex: Longman)

[2] Reeder R J 1983 Crystal chemistry of rhombohedral carbonates *Carbonates: Mineralogy and Chemistry (Reviews in Mineralogy, vol 11)* ed R J Reeder (Washington, DC: Mineralogical Society of America)

[3] Bucci C and Fieschi R 1964 *Phys. Rev. Lett.* **12** 16

[4] Papathanassiou A N and Grammatikakis J 1997 *Phys. Rev.* B **56** 8590

[5] Papathanassiou A N and Grammatikakis J 1996 *Phys. Rev.* B **53** 16 253

[6] Papathanassiou A N, Grammatikakis J, Katsika V and Vassilikou-Dova A B 1995 *Radiat. Effects Defects Solids* **134** 247

[7] Bogris N, Grammatikakis J and Papathanassiou A N 1998 *Phys. Rev.* B **58** 10 319

[8] Papathanassiou A N and Grammatikakis J 2000 *J. Phys. Chem. Solids* **61** 1633

[9] Papathanassiou A N and Grammatikakis J 1997 *J. Phys. Chem. Solids* **58** 1063

[10] Papathanassiou A N 1999 *J. Phys. Chem. Solids* **60** 407

[11] Vila R and Jimenez de Castro M 1992 *J. Phys. D: Appl. Phys.* **25** 1357

[12] van Beek L K H 1967 Dielectric behavior of heterogeneous systems *Progress in Dielectrics* vol 7, ed J B Birks (London: Heywood) p 69

[13] Hanai T 1968 Electrical properties of emulsions *Emulsion Science* ed F Sherman (New York: Academic)

[14] Calame J P, Fontanella J J, Wintersgill M C and Andeen C 1985 *J. Appl. Phys.* **58** 2811

[15] Papathanassiou A N and Grammatikakis J 2000 *Phys. Rev.* B **61** 16 514

[16] van Turnhout J 1980 Thermally stimulated discharge of polymers *Electrets* ed G M Sessler (Berlin: Springer)

[17] Nedetzka T, Reichle M, Mayer A and Vogel H 1970 *J. Phys. Chem.* **74** 2652

[18] Zielinski M and Kryszewski M 1977 *J. Electrostatics* **3** 69

[19] Schrader S and Carius H-E 1991 *Proc. 7th Int. Symp. on Electrets ISE7 (Berlin, 1991)* ed R Gerhard-Multhaupt *et al*, p 581

[20] Papathanassiou A N, Grammatikakis J and Bogris N 1993 *Phys. Rev.* B **48** 17 715

[21] Papathanassiou A N 2000 *J. Phys.: Condens. Matter* **12** 9985

[22] Müller P 1981 *Phys. Status Solidi* a **67** 11

[23] Angenheister G (ed) 1982 Group V *Landolt-Börnstein Tables* vol 1b (Berlin: Springer)

[24] Papathanassiou A N 1995 Dielectric relaxation and transport phenomena under pressure in natural rare earth carbonate salts *PhD Dissertation* University of Athens